Noninvasive Magnetic Resonance Spectroscopic Pharmacodynamic Markers of the Choline Kinase Inhibitor MN58b in Human Carcinoma Models

Nada M.S. Al-Saffar,[1] Helen Troy,[3] Ana Ramírez de Molina,[4] Laura E. Jackson,[1] Basetti Madhu,[3] John R. Griffiths,[3] Martin O. Leach,[1] Paul Workman,[2] Juan C. Lacal,[4] Ian R. Judson,[2] and Yuen-Li Chung[3]

[1]Cancer Research UK Clinical Magnetic Resonance Research Group, The Institute of Cancer Research and The Royal Marsden NHS Foundation Trust; [2]Cancer Research UK Center for Cancer Therapeutics, The Institute of Cancer Research, Sutton, Surrey, United Kingdom; [3]Cancer Research UK Biomedical Magnetic Resonance Research Group, Department of Basic Medical Sciences, St. George's University of London, London, United Kingdom; and [4]Translational Oncology Unit, Department of Molecular and Cellular Biology of Cancer, Instituto de Investigaciones Biomédicas, Madrid, Spain

Abstract

MN58b is a novel anticancer drug that inhibits choline kinase, resulting in inhibition of phosphocholine synthesis. The aim of this work was to develop a noninvasive and robust pharmacodynamic biomarker for target inhibition and, potentially, tumor response following MN58b treatment. Human HT29 (colon) and MDA-MB-231 (breast) carcinoma cells were examined by proton (^{1}H) and phosphorus (^{31}P) magnetic resonance spectroscopy (MRS) before and after treatment with MN58b both in culture and in xenografts. An *in vitro* time course study of MN58b treatment was also carried out in MDA-MB-231 cells. In addition, enzymatic assays of choline kinase activity in cells were done. A decrease in phosphocholine and total choline levels ($P < 0.05$) was observed *in vitro* in both cell lines after MN58b treatment, whereas the inactive analogue ACG20b had no effect. In MDA-MB-231 cells, phosphocholine fell significantly as early as 4 hours following MN58b treatment, whereas a drop in cell number was observed at 48 hours. Significant correlation was also found between phosphocholine levels (measured by MRS) and choline kinase activities ($r^2 = 0.95$, $P = 0.0008$) following MN58b treatment. Phosphomonoesters also decreased significantly ($P < 0.05$) in both HT29 and MDA-MB-231 xenografts with no significant changes in controls. ^{31}P-MRS and ^{1}H-MRS of tumor extracts showed a significant decrease in phosphocholine ($P \leq 0.05$). Inhibition of choline kinase by MN58b resulted in altered phospholipid metabolism both in cultured tumor cells and *in vivo*. Phosphocholine levels were found to correlate with choline kinase activities. The decrease in phosphocholine, total choline, and phosphomonoesters may have potential as noninvasive pharmacodynamic biomarkers for determining tumor response following treatment with choline kinase inhibitors. (Cancer Res 2006; 66(1): 427-34)

Introduction

Choline kinase (ATP/choline phosphotransferase, EC 2.7.1.32) catalyzes the phosphorylation of choline by ATP in the presence of Mg^{2+}, yielding phosphocholine (1). This enzyme step commits choline to the Kennedy pathway (cytidylyl diphosphate-choline pathway) for the biosynthesis of phosphatidylcholine, the major phospholipid constituent in biomembranes. Phosphatidylcholine has an essential structural function as well as serving as a reservoir for lipid second messengers (e.g., lyso-phosphatidylcholine, phosphatidic acid, diacylglycerol, and lyso-phosphatidic acid; ref. 2). The cytidylyltriphosphate:phosphocholine cytidylyltransferase reaction is commonly referred to as the rate-limiting step in phosphatidylcholine biosynthesis (3). There is evidence that phosphorylation by choline kinase is also a slow step and can be regulatory for phosphatidylcholine biosynthesis, where increased choline kinase activity results in a corresponding increase in the rate of phosphatidylcholine biosynthesis (4).

Increased activity of choline kinase has been reported to be associated with an enhanced generation of phosphocholine, mostly independent of the rate of net phosphatidylcholine biosynthesis. Growth factors (5, 6), chemical carcinogens (7, 8), and/or *ras* oncogene transfection (9, 10) have been shown to cause induction of choline kinase activity, leading to an accumulation of phosphocholine. Furthermore, microinjection of phosphocholine into cells resulted in increased mitogenesis (6). Recently, increased choline kinase activity has been shown in human tumor-derived cell lines and in a variety of human tumors compared with their corresponding normal tissues (11, 12). These findings strongly support the role of choline kinase in tumor transformation and carcinogenesis, suggesting choline kinase as a potential target for the development of anticancer drugs.

A novel molecular therapeutic strategy focused on choline kinase inhibition has been developed recently, resulting in the discovery of a group of compounds with an inhibitory activity against choline kinase (13–15). MN58b (1,4-[4-4′-Bis-{[4-(dimethylamine)pyridinium-1-yl] methyl}diphenyl]butane dibromide) exhibits selective inhibition of choline kinase, inhibits proliferation of cancer cells *in vitro*, and displays therapeutic activity against human tumor xenografts *in vivo* (14, 16–19).

The rational development of new molecular cancer therapeutics requires the discovery and validation of biomarkers of drug action (20–22). These are valuable because they can provide proof of concept for the intended mechanism of action in phase I clinical studies, as well as aiding dose selection for phase II trials. A recent study has shown that in the majority of phase I trial designs for solid tumor studies of targeted, noncytotoxic agents, traditional end points rather than molecular measures of drug effects are used for selection of the recommended phase II dose (23). The

Note: P. Workman is a Cancer Research UK Life fellow.

Requests for reprints: Martin O. Leach, Cancer Research UK Clinical Magnetic Resonance Research Group, The Institute of Cancer Research, The Royal Marsden NHS Foundation Trust, Downs Road, Sutton, Surrey SM2 5PT, United Kingdom. Phone: 44-20-8661-3338; Fax: 44-20-8661-0846; E-mail: martin.leach@icr.ac.uk.

doi:10.1158/0008-5472.CAN-05-1338

development of surgically noninvasive end points is particularly important because it avoids the need for tumor biopsy.

Magnetic resonance spectroscopy (MRS) is increasingly used for the study of cellular metabolism, both *in vivo* (small animals and humans) and *in vitro* (body fluids, tissue cultures, tissue extracts, and isolated tissues). MRS offers several advantages for metabolic studies, being noninvasive and nondestructive, enabling serial measurements of intact tissues. A further advantage of MRS is the identification and quantification of multiple tissue metabolites from a single spectrum. MRS has been applied to the characterization of neoplastic and normal human tissues (24, 25), early detection of therapeutic response (26, 27), drug development (28), and the identification of metabolic changes associated with apoptosis (29, 30). Using MRS, higher levels of phosphomonoesters comprising phosphocholine and phosphoethanolamine were observed in tumors compared with the corresponding normal tissues (31, 32). Other MRS studies showed that progression from the normal to the malignant phenotype is associated with an increase in both phosphocholine and total choline–containing metabolites (33, 34). Furthermore, a MRS study detected an increase in phosphocholine levels in NIH3T3 cells transfected with mutant *ras* oncogene compared with the parental cell line (35).

To identify a noninvasive and robust biomarker for choline kinase inhibition and potentially tumor response following MN58b treatment, we did comprehensive proton (^{1}H) and phosphorus (^{31}P) MRS studies in human carcinoma models. ^{1}H-MRS and ^{31}P-MRS evaluation of extracts of two human carcinoma cell lines [MDA-MB-231 (breast) and HT29 (colon)] were used to determine whether any MR spectral changes were associated with choline kinase inhibition after MN58b treatment. We have also examined the effect of MN58b on MDA-MB-231 and HT29 xenograft models to show therapeutic efficacy, to determine whether MRS changes observed in the cell studies were reproducible *in vivo*, and to investigate whether ^{1}H-MRS and ^{31}P-MRS could provide a noninvasive pharmacodynamic biomarker for the therapeutic action of choline kinase inhibitors in clinical trials.

Materials and Methods

Materials. MN58b (6 mmol/L) dissolved in saline and ACG20b (α-α′-Bis(4-piperidine pyridinium-1-yl)P-xilene dibromide; 2.67 mmol/L) dissolved in double deionized water have been previously described (14, 16). Both drugs are produced at Prof. Lacal's laboratories and are not available as commercial compounds. DMEM, FCS, penicillin, and streptomycin were purchased from Life Technologies (Paisley, United Kingdom). Perchloric acid and potassium hydroxide (KOH) were purchased from Merck (Poole, United Kingdom). Hypnorm was purchased from Jansen Pharmaceuticals (Buckinghamshire, United Kingdom), and Hypnovel was purchased from Roche (Welwyn Garden City, United Kingdom). All other chemicals were purchased from Sigma (Poole, United Kingdom).

Cell culture and treatment. MDA-MB-231 and HT29 cancer cell lines (American Type Culture Collection, Manassas, VA) were cultured in DMEM supplemented with 10% FCS, 80 units/mL penicillin, and 80 μg/mL streptomycin at 37°C in 5% CO_2. Cell growth inhibition (96 hours) for MDA-MB-231 cells with seeding density of 1×10^3 in 200 μL using 96-well plates, was measured by sulforhodamine B assay to assess IC_{50} (36). MDA-MB-231 cells were treated with MN58b at pharmacologically active concentrations corresponding to $5 \times IC_{50}$ (6 μmol/L) for 4, 13, 19, 30, and 48 hours or 6 μmol/L ACG20b (an inactive analogue) for 48 hours at 37°C, and HT29 cells were treated with 2.5 μmol/L MN58b or 2.5 μmol/L ACG20b for 48 hours at 37°C. The cells then underwent trypsinization and trypan blue exclusion assay (37). The effect of treatment on cell number was monitored by counting the number of attached cells in a treated flask and comparing that number with the number of attached cells in a control flask.

Cell cycle analysis. Cell cycle analysis of attached and detached control and treated cells was done on cells (1×10^6) fixed in 70% ethanol, treated with 100 μg/mL RNase A in citrate-buffered saline for 30 minutes at 37°C, and stained with 4 μg/mL propidium iodide (38), using an Elite Enhanced System Performance cell sorter (Beckman Coulter, High Wycombe, United Kingdom) at 488 nm. The cytometry data were analyzed using the WinMdi and Cylchred software (University of Wales College of Medicine, Cardiff, United Kingdom).

HT29 and MDA-MB-231 tumor xenograft models. MF-1 nude mice were injected s.c. in the flank with 0.2 mL of a suspension of HT29 human colon carcinoma cells (2.5×10^7/mL) or MDA-MB-231 human breast carcinoma cells (5×10^7/mL) that had been grown as a monolayer in cell culture (37). Tumor size was calculated by measuring the length, width, and depth of each tumor using calipers and by using the following formula: $l \times w \times d \times (\pi/6)$. Once an appropriate tumor size (approximate volume of 500 mm^3) was established, mice were randomly divided into two groups: one group was treated with MN58b in saline at 4 mg/kg i.p. once a day for 5 days, and one group was treated with saline alone following the same regimen. Animals were treated in accordance with local and national ethical requirements and with the United Kingdom Coordinating Committee on Cancer Research Guidelines for the Welfare of Animals in Experimental Neoplasia (39).

***In vitro* ^{1}H-MRS and ^{31}P-MRS of cell extracts.** To obtain an MR spectrum, 1×10^7 to 2×10^7 cells in logarithmic phase were extracted from cell culture, as previously described (30, 40). Briefly, cells were rinsed with ice-cold saline and fixed with 6 mL of ice-cold methanol. Cells were then scraped off the surface of the culture flask, collected into tubes, and vortexed for 30 seconds at room temperature to optimize phospholipid metabolite extraction from the ruptured cells. Chloroform (6 mL) was then added to each tube followed by an equal volume of deionized water. Following phase separation, the solvent in the upper methanol/water phase was removed using a freeze dryer, and the lipid metabolites were recovered by evaporation of chloroform to dryness (30, 40), and samples were stored at −80°C until analysis. Before acquisition of the MRS spectra, the water-soluble metabolites were resuspended in deuterium oxide (D_2O) for ^{1}H-MRS or D_2O with 10 mmol/L EDTA (pH 8.2) for ^{31}P-MRS, and the lipid metabolites were resuspended in deuteriated chloroform for ^{1}H-MRS. ^{1}H-MRS and ^{1}H-decoupled ^{31}P-MRS spectra were acquired at room temperature on a 500 MHz Bruker spectrometer (Bruker Biospin, Coventry, United Kingdom) using a 30-degree flip angle, a 1-second relaxation delay, spectral width of 100 ppm, and 32 K data points for ^{31}P; a 30-degree flip angle, a 1-second relaxation delay, spectral width of 12 ppm, and 32 K data points for ^{1}H (lipids); and a 90-degree flip angle, a 1-second relaxation delay, spectral width of 12 ppm, 64 K data points, and HDO resonance suppression by presaturation for ^{1}H (aqueous). Metabolite contents were determined by integration and normalized relative to the peak integral of an internal reference [0.15% 3-(trimethylsilyl)propionic-2,2,3,3-d_4 acid sodium salt (water fractions) or 0.03% tetramethylsilane (lipid fractions) for ^{1}H-MRS, and methylene diphosphonic acid (70 μL, 2 mmol/L) for ^{31}P-MRS] and corrected for signal intensity saturation and the number of cells extracted per sample.

***In vivo* ^{31}P-MRS of HT29 and MDA-MB-231 tumor xenografts.** Animals were anesthetized with a single i.p. injection of a Hypnovel/Hypnorm/water (1:1:2) mixture as previously described (37). Animals were placed in the bore of a Varian 4.7-T nuclear magnetic resonance (NMR) spectrometer at St. George's University of London, and tumors were positioned in the center of a 12-mm two-turn ^{1}H/^{31}P surface coil. Image-selected *in vivo* spectroscopy–localized ^{31}P-MR spectra of the tumors were obtained at 37°C, as previously described (41). Briefly, a gradient strength of up to 7.5×10^{-4} T/cm was applied with adiabatic pulses of 800 milliseconds, a 90-degree sincos excitation pulse, and a sech 180 inversion pulse, with a total repetition time of 3 seconds and 600 averages. ^{31}P-MRS of the tumors was carried out before treatment (i.e., day 1) and 4 days after treatment (i.e., day 5). ^{31}P-MR spectra were quantified using the VARiable PROjection program to determine precise chemical shifts and peak integrals

as previously described (42). After the final ^{31}P-MRS study, tumors were freeze clamped and stored at −80°C until analysis.

The surface coils used to obtain the ^{31}P-MRS signal from s.c. tumors *in vivo* were of nonuniform spatial sensitivity; thus, it is not possible to use an internal standard. Thus, the signal intensities observed in the *in vivo* ^{31}P-MR spectra are expressed as ratios of metabolites.

***In vivo* ^{1}H-MRS of HT29 tumor xenografts.** Anesthetized mice were placed in the MR system as described above. Voxels were selected from scout gradient echo images, and localized shimming yielded line widths of the order of 20 to 30 Hz. The PRESS localization method with water suppression was used to detect choline with a repetition time of 2 seconds, 64 transients, and echo times of 20, 68, 136, 272, and 408 milliseconds. For unsuppressed water, 16 transients were acquired with the same acquisition variables as above except with a lower receiver gain. After the final ^{1}H-MRS study, tumors were freeze clamped and stored at −80°C until analysis.

MRUI software (42) was used for all spectral processing programs, including preprocessing, fitting, and quantification of peak areas of the observed metabolites. Eddy current correction was done by using the water FID to phase correct the metabolite signal point by point (43). This corrects the phase of the spectrum without any subjective bias. The last 100 data points were used to calculate root-mean-square noise and correct for direct current offsets. Using the choline and water peak areas as a function of echo time, choline and water T_2 curves were fitted to a single exponential decay function and choline, and water intercepts (M_0) and T_2s were derived from these fits. The Levenberg-Marquardt algorithm was used for optimization. The choline concentration was calculated using tumor water as a reference assuming tumor tissue water was 80% (44 mol/L; ref. 44) and according to the equation:

$$[\text{choline}] = (\text{choline/water})_{\text{TE}=0} \times W_C \times (N_W/N_C) \times (AV_n \times RG_c)$$

where [choline] = choline concentration, $(\text{choline/water})_{\text{TE}=0}$ = ratio of choline peak area and water peak area (calculated at TE = 0 from individual T_2 fits), W_c = water concentration (44 mol/L), N_w = number of protons in water = 2, N_c = number of protons in choline = 9, AV_n = normalization factor for number of averages, and RG_c = receiver gain correction factor. The corrections for the number of averages and receiver gains were required because they are different for the acquisition of water and metabolite spectra. This method has been validated using a phantom solution with a known concentration of phosphocholine, and the calculated error of our measurements using this method was found to be about 3%.

***In vitro* ^{31}P-MRS of tumor extracts.** The freeze-clamped tumors were extracted in 6% perchloric acid, as previously described (45). Neutralized extracts were freeze-dried and reconstituted in 1 mL D_2O, and the extracts (0.5 mL) were placed in 5-mm NMR tubes. For ^{1}H-MRS, the water resonance was suppressed by using gated irradiation centered on the water frequency. 3-(trimethylsilyl)propionic-2,2,3,3-d_4 acid sodium salt (50 μL, 5 mmol/L) was added to the samples for chemical shift calibration and quantification. Immediately before the MRS analysis, the pH of the samples was readjusted to 7 with perchloric acid or KOH. For ^{31}P-MRS, which was carried out after the ^{1}H-MRS study, EDTA (50 μL, 60 mmol/L) was added to each sample for chelation of metals ions, and methylene diphosphonic acid (50 μL, 5 mmol/L) was added to each sample for chemical shift calibration and quantification. The extract spectra for both the control and the treated animals were acquired under identical conditions.

Enzymatic assays of choline kinase activity in cell extracts. Following 4, 13, 19, 30, and 48 hours of treatment with 6 μmol/L MN58b, exponentially growing cells from three p60 plates (1×10^6) were lysed in 80 μL of lysis buffer [1.5 mmol/L $MgCl_2$, 0.2 mmol/L EDTA, 0.3 mol/L NaCl, 25 mmol/L HEPES (pH 7.5), 20 mmol/L β-glycerophosphate, and 0.1% Triton X-100] to a final concentration of 3 μg/μL. From this, 90 μg of total protein were used per point as source of choline kinase in buffer containing 100 mmol/L Tris-HCl (pH 8), 100 mmol/L $MgCl_2$, and 10 mmol/L ATP, as previously described (11).

Statistical analysis. Data are presented as the mean ± SD, and $n \geq 3$ unless otherwise specified. For comparison of metabolite concentrations and ratios, unpaired two-tailed Student's standard *t* tests were used with a $P \leq 0.05$ considered statistically significant. The Mann-Whitney *U* test was done for comparison of proportions, with a $P \leq 0.05$ considered statistically significant. Regression correlation was used to correlate changes in phosphocholine levels (by MRS) and choline kinase activities.

Results

Cellular effects of MN58b treatment. MDA-MB-231 and HT29 cells were treated with MN58b at pharmacologically active concentrations corresponding to 5 × IC_{50} obtained by the 96 hours of sulforhodamine B assay (6 and 2.5 μmol/L, respectively) for 4, 13, 19, 30, and 48 hours (MDA-MB-231) and 48 hours (HT29). After 48 hours of incubation, the number of MN58b treated cells per flask as a % of control showed a statistically significant reduction to 78 ± 10% ($P < 0.04$) in MDA-MB-231 (Fig. 1*A*) and 48 ± 5% ($P < 0.01$) in HT29, consistent with decreased proliferation. In contrast, following treatment with the inactive analogue ACG20b, cell number was similar to controls (95 ± 8%, $P = 0.5$) and (95 ± 7%, $P = 0.4$) in MDA-MB-231 and HT29 respectively. To further characterize the cellular effects of MN58b, cell cycle distribution following MN58b treatment was determined by flow cytometry on attached cells. No statistically significant effect on the cell cycle distribution was seen in MDA-MB-231 cells following treatment with MN58b for up to 30 hours. However, at 48 hours, the percentage of cells in G_1 phase showed a statistically significant increase from 43 ± 4% to 54 ± 3% ($P = 0.01$), whereas the percentage of cells in S and G_2 phases showed a statistically significant decrease from 43 ± 3% to 35 ± 4% ($P = 0.02$) and from 14 ± 1% to 11 ± 1% ($P = 0.01$), respectively. For HT29 cells, 48 hours of treatment with MN58b also caused a statistically significant increase in the percentage of cells in G_1 phase from 60 ± 4% to 80 ± 2% ($P = 0.007$), and the percentage of cells in S and G_2 phases decreased statistically significantly from 32 ± 4% to 17 ± 3% ($P = 0.02$) and from 8 ± 2% to 3 ± 1% ($P = 0.04$), respectively. On the other hand, 48 hours of treatment with the inactive analogue ACG20b had no statistically significant effect on the cell cycle distribution in both MDA-MB-231 and HT29 cells ($P = 0.4$; data not shown).

***In vitro* ^{1}H-MRS and ^{31}P-MRS of cell extracts.** MRS of carcinoma cells treated *in vitro* with MN58b was used to identify potential noninvasive markers of choline kinase inhibition. Figure 1*B* illustrates the ^{31}P-MR spectra of control and 48-hour MN58b-treated MDA-MB-231 cells. Detailed analysis of ^{31}P-MR spectra of control and MN58b-treated MDA-MB-231 cells at 4, 13, 16, 30, and 48 hours showed that MN58b treatment led to a statistically significant time-dependent drop in phosphocholine levels relative to controls which started as early as 4 hours (81 ± 6%, $P = 0.04$) and was down to 40 ± 2% ($P = 0.00001$) at 48 hours relative to controls (Fig. 1*A*). A statistically significant drop in phosphocholine (42 ± 13%, $P = 0.03$) relative to control was also detected following 48 hours incubation of HT29 cells with MN58b (Fig. 1*C*). Changes in other ^{31}P-MR detectable metabolites (glycerophosphoethanolamine, glycerophosphocholine, and nucleotide triphosphates) were not statistically significant in either cell line ($P > 0.05$). It was not possible to accurately measure phosphoethanolamine levels in cell extracts due to the very small phosphoethanolamine signal in both cell lines.

^{31}P-MR spectra of MDA-MB-231 and HT29 cells treated with ACG20b, the inactive analogue, were also investigated to verify that the ^{31}P-MRS detected drop in phosphocholine is due to the inhibitory effect of MN58b on choline kinase. No statistically significant change in phosphocholine levels was observed in MDA-MB-231 (88 ± 11%, $P = 0.2$) or HT29 (88 ± 10%, $P = 0.2$) cells

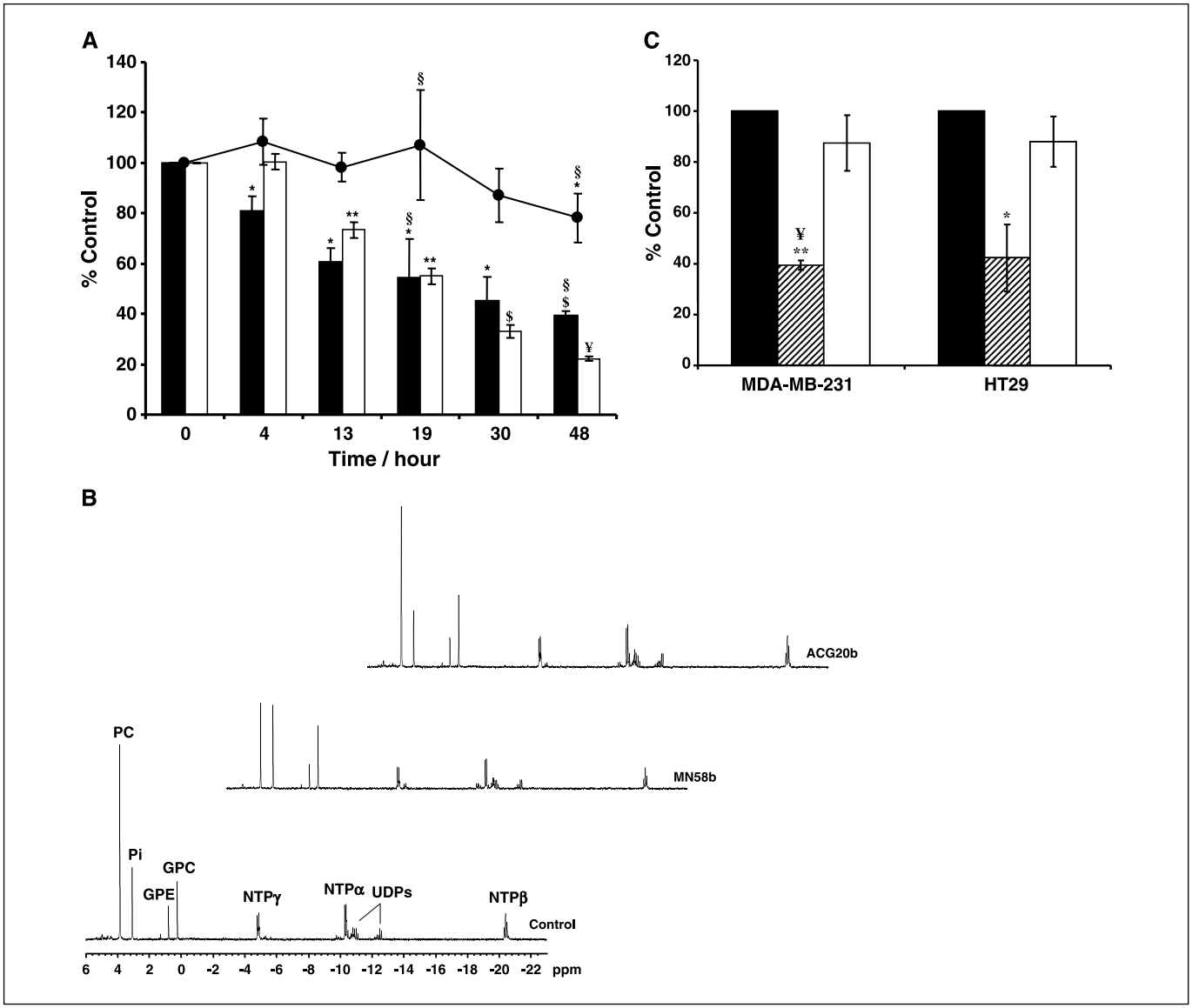

Figure 1. Inhibition of choline kinase with MN58b (6 μmol/L) but not ACG20b is associated with a drop in cellular proliferation, phosphocholine levels, and choline kinase activity in MDA-MB-231 cells. *A,* % (relative to control) cell density (●), phosphocholine (*PC*) levels by MRS (*solid columns*), and choline kinase activity (*open columns*) in MDA-MB-231 breast carcinoma cells following treatment with MN58b (6 μmol/L) for the indicated times. *, $P < 0.04$; **, $P < 0.001$; $, $P < 0.00002$; ¥, $P = 0.0000003$ (statistically significant different from the control); two-tailed unpaired *t* test was used for all comparisons. *Columns,* mean of three separate experiments unless otherwise stated (§, $n = 4$); *bars,* SD. —●—, cell no.; ▬, PC; ▭, pmol PC/μg prot/min. *B, in vitro* ^{31}P-MRS of an MDA-MB-231 cell extract without treatment (*bottom*), or following treatment with MN58b (*middle*), or inactive analogue ACG20b (*top*). Peak assignments were as follows: phosphocholine (*PC*), inorganic phosphate (P_i), glycerophosphocholine (*GPC*), glycerophosphoethanolamine (*GPE*), nucleoside triphosphate (*α-NTP, β-NTP, γ-NTP*), uridine triphosphate sugars (*UDPs*). Confirmed in four separate experiments. Representative spectra. *C,* % (relative to control) phosphocholine levels in MDA-MB-231 breast and HT29 colon carcinoma cells without treatment (*solid columns*), or following treatment with MN58b (*hatched columns*), or ACG20b (*open columns*) for 48 hours. *, $P = 0.03$; **, $P = 0.00001$ (statistically significantly different from the control); two-tailed unpaired *t* test was used for all comparisons. *Columns,* mean of three separate experiments unless otherwise stated (¥, $n = 4$); *bars,* SD. ■, control; ▨, MN58b; □, ACG20b.

following 48 hours of treatment with ACG20b (Table 1; Fig. 1*B* and *C*). Changes in phosphocholine concentrations in MDA-MB-231 cells after a time course of treatment with MN58b are summarized in Table 1 and Fig. 1*A*.

^{1}H-MR spectra of extracts of control and MN58b-treated MDA-MB-231 cells at 4, 13, 19, 30, and 48 hours were also investigated. A statistically significant time-dependent drop in the total choline content (choline + phosphocholine + glycerophosphocholine) was observed following 19 hours of incubation with MN58b (63 ± 17%, $P = 0.03$) relative to control, decreasing to 49 ± 9% ($P = 0.002$) at 48 hours following MN58b treatment. The decrease in total choline was similar to the drop in phosphocholine levels measured by ^{31}P-MRS; hence, the decrease in the total choline is due to the drop in phosphocholine, whereas intracellular choline and glycerophosphocholine levels were not affected by MN58b treatment.

Phosphocholine is required for the synthesis of phosphatidylcholine. Hence, to find out whether the drop in phosphocholine would cause a similar drop in the phosphatidylcholine levels, ^{1}H-MR spectra of the lipid fractions of control and MN58b-treated MDA-MB-231 and HT29 cells were measured. No significant changes in phosphatidylcholine levels [using the $N(CH_3)_3$ peak

Table 1. Phosphocholine levels (measured by *in vitro* ^{31}P-MRS) and choline kinase activities in control and treated MDA-MB-231 cell extracts

Time (h)	Concentration of PC by ^{31}P-MRS (fmol/cell)		ChoK activity (pmol PC/ μg protein/min)
	Control	Treated	
MN58b			
0	*	*	276.0 ± 9.3
4	46.9 ± 3.8	37.8 ± 3.1 †	277.2 ± 9.6
13	51.9 ± 2.2	31.4 ± 3.1 ‡	202.1 ± 9.0§
19	46.2 ± 4.4‖	24.6 ± 5.1 ‡,‖	152.8 ± 7.5¶
30	44.0 ± 0.8	20.0 ± 4.1 ‡	91.1 ± 7.9¶
48	36.0 ± 6.6‖	14.1 ± 2.0 ‡,‖	61.2 ± 2.3¶
ACG20b			
48	31.9 ± 2.7	27.7 ± 1.8	—

NOTE: Data are expressed as the mean ± SD.
Abbreviations: PC, phosphocholine; ChoK, choline kinase.
*PC concentrations not calculated for 0-hour exposure to MN58b as all time points compare treated cells and untreated controls.
†Two-tailed unpaired *t* test was used to compare PC changes in control and treated cells within the same time-point with $P = 0.06$.
‡Two-tailed unpaired *t* test was used to compare PC changes in control and treated cells within the same time-point with $P < 0.01$.
§Two-tailed unpaired *t* test was used to compare changes in ChoK activities at 0 hour (control) with various time-points following MN58b treatment with $P < 0.0001$.
‖$n = 4$ (others, $n = 3$).
¶Two-tailed unpaired *t* test was used to compare changes in ChoK activities at 0 hour (control) with various time-points following MN58b treatment with $P < 0.000001$.

resonating at 3.32 ppm] were detected following treatment of both cell lines with MN58b ($P > 0.4$; data not shown). These results are consistent with previous findings using NIH3T3 cells (18) and human primary lymphocytes (19).

Choline kinase activities in cell extracts and correlation to phosphocholine levels measured by MRS. ^{14}C choline labeling was used as a measure of choline kinase activity in MDA-MB-231 cells after a time course treatment with MN58b (Table 1; Fig. 1*A*). Significant correlation was found between phosphocholine concentrations (measured by MRS) and choline kinase activities ($r^2 = 0.95$, $P = 0.0008$).

***In vivo* ^{1}H-MRS and ^{31}P-MRS of HT29 xenografts.** In this study, MN58b inhibited tumor growth in HT29 xenografts by 70% (% treated versus control, % T/C), confirming previous findings (16).

In vivo ^{1}H-MR and ^{31}P-MR spectra from a HT29 tumor pre-MN58b and post-MN58b treatment are shown in Fig. 2*A* to *D*. Statistically significant decreases in the total choline concentration ($P = 0.01$) and phosphomonoester/total phosphorus signal ratio ($P = 0.05$) were also observed post-MN58b treatment (Table 2A). No statistically significant change in total choline concentration was observed in the control (vehicle treated) tumor group. A statistically significant increase in phosphomonoester/total phosphorus signal ratio ($P = 0.04$) was observed in the control group.

***In vivo* ^{31}P-MRS of MDA-MB-231 xenografts.** Previous studies have shown statistically significant growth delays when MDA-MB-231 human breast carcinoma xenografts were treated with MN58b (17). Consistent with these results, we found that MN58b treatment for 5 days inhibited tumor growth by 85% (%T/C).

In vivo ^{31}P-MRS of the MDA-MB-231 tumors showed statistically significant decreases in the phosphomonoester/total phosphorus signal ratio ($P = 0.05$) following MN58b treatment (Table 2B). No statistically significant change was observed in the control (vehicle treated) tumor group.

***In vitro* ^{31}P-MRS of HT29 and MDA-MB-231 tumor extracts.** *In vitro* ^{31}P-MRS analysis of extracts of the HT29 and MDA-MB-231 tumor xenografts allows better resolution of the phosphomonoester signal than is possible *in vivo*. Reduced levels of phosphocholine ($P = 0.03$ and $P = 0.04$, respectively) were seen in MN58b-treated tumors (Table 3A), confirming our *in vivo* ^{31}P-MRS and ^{1}H-MRS findings. No statistically significant change in

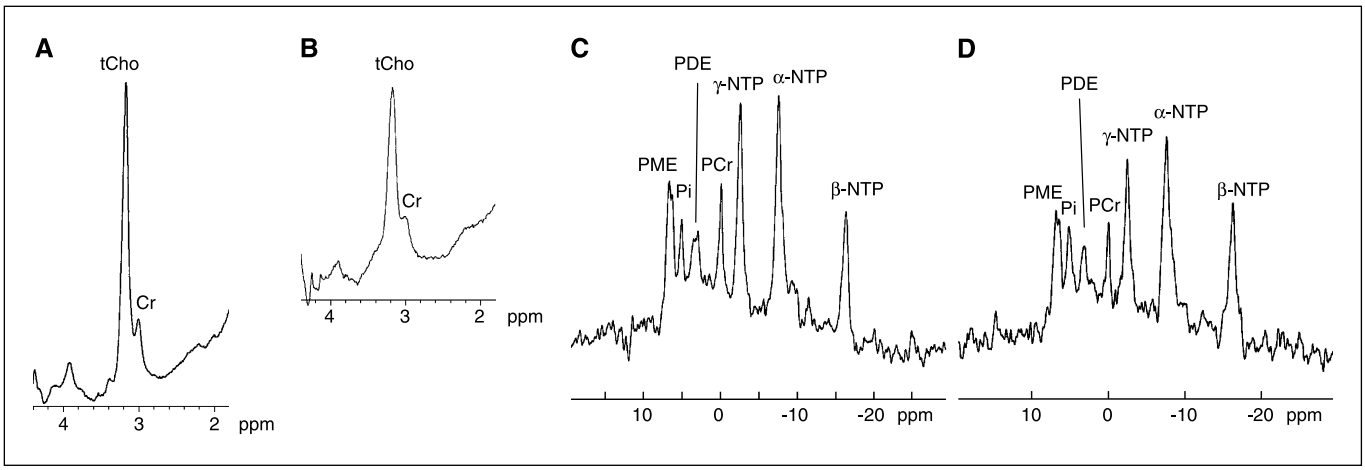

Figure 2. Statistically significant decreases in the total choline concentration and phosphomonoesters/total phosphorus signal ratio were found in HT29 xenografts following MN58b treatment. *In vivo* proton (^{1}H)-MRS of a HT29 tumor before (*A*) and after (*B*) MN58b treatment. *In vivo* phosphorus (^{31}P)-MRS of a HT29 tumor before (*C*) and after (*D*) MN58b treatment. Peak assignments were as follows: phosphomonoesters (*PME*), phosphodiesters (*PDE*), inorganic phosphate (P_i), phosphocreatione (*PCr*), nucleoside triphosphate (*α-NTP, β-NTP, γ-NTP*), total choline (*tCho*), creatine (*Cr*). Confirmed in seven (^{31}P-MRS) and five (^{1}H-MRS) separate experiments. Representative spectra.

Table 2. *In vivo* MRS of HT29 tumors and MDA-MB-231 tumors

Metabolite ratio	Pre-MN58b	Post-MN58b	*P**
A. HT29 tumors pre-MN58b and post-MN58b treatment†			
^{31}P-MRS (n = 7)			
PME/P_{tot}	0.21 ± 0.02	0.17 ± 0.02	0.05
β-NTP/P_{tot}	0.18 ± 0.01	0.20 ± 0.01	0.23
β-NTP/P_i	2.81 ± 0.35	2.94 ± 0.67	0.81
P_i/P_{tot}	0.07 ± 0.01	0.09 ± 0.02	0.34
^{1}H-MRS (n =5)			
Total choline (mmol/L)	10.11 ± 0.88	7.61 ± 0.60	0.01
B. MDA-MB-231 tumors (n = 10) pre-MN58b and post-MN58b treatment†			
PME/P_{tot}	0.24 ± 0.01	0.20 ± 0.02	0.05
β-NTP/P_{tot}	0.17 ± 0.01	0.19 ± 0.01	0.14
β-NTP/P_i	1.57 ± 0.23	2.09 ± 0.31	0.22
P_i/P_{tot}	0.13 ± 0.01	0.11 ± 0.01	0.38

Abbreviations: PME, phosphomonoester; P_{tot}, total phosphorus signal; β-NTP, β-nucleoside triphosphate; P_i, inorganic phosphate.
*Two-tailed paired t-test was used to compare changes pre-MN58b and post-MN58b treatment within the same group of animals.
†Data are expressed as the mean ± SE.

phosphoethanolamine, glycerophosphoethanolamine, and glycerophosphocholine levels relative to controls was found in either xenograft model (Table 3).

***In vitro* ^{1}H-MRS of HT29 and MDA-MB-231 tumor extracts.** Expanded *in vitro* ^{1}H-MR spectra (i.e., 3.1-3.5 ppm) of the HT29 tumor extracts from a control vehicle-treated and a MN58b-treated mouse are illustrated in Fig. 3*A* and *B*, respectively, showing resonances from free choline, phosphocholine, glycerophosphocholine, and taurine. The level of phosphocholine was found to be significantly decreased in both MN58b-treated HT29 ($P \leq 0.05$) and MDA-MB-231 ($P \leq 0.05$) tumor extracts when compared with vehicle-treated tumor extracts (Table 3B), confirming our *in vivo* MRS findings. No significant changes in free choline and glycerophosphocholine levels were found following MN58b treatment in either tumor model.

Discussion

Anticancer drug research is increasingly focusing on specific molecular targets responsible for the malignant phenotype (20, 46), with the ultimate goal of improving activity and therapeutic selectivity for tumor versus normal cells. Choline kinase has been implicated in cell proliferation, playing an important role in mitogenic signal transduction pathways (9, 14, 15). Furthermore, increased levels of choline kinase activity and phosphocholine production have been observed in human cancers (11, 12). These observations have resulted in the development of a therapeutic strategy focused on choline kinase inhibition (13–15).

MN58b is a potent choline kinase inhibitor (13, 16–19). The mechanism of action and tumor response to MN58b have been assessed using molecular markers and biochemical assays, especially the selective inhibition of choline kinase and consequently depletion of phosphocholine (16–19). However, a noninvasive direct or surrogate marker of target inhibition and potentially of tumor response to this novel treatment would be a valuable aid to the clinical development of choline kinase inhibitors. We investigated MRS for potential markers of drug activity in two human carcinoma cell lines [MDA-MB-231 (breast) and HT29 (colon)] both in cell culture and in xenograft mouse models. A statistically significant drop in phosphocholine levels (phosphomonoester *in vivo*) has been observed in cultured cells and in solid tumors of both tumor lines following MN58b treatment. *In vivo* measurement of phosphomonoester includes both phosphocholine and phosphoethanolamine peaks, which could be separated at high field or by using ^{1}H decoupling. No effect on other ^{31}P-MR detectable metabolites was found. These MRS changes, suggesting inhibition of choline kinase, are consistent with the proposed mechanism of action of MN58b (16, 18, 19). Our data are also consistent with a recent study on choline kinase inhibition by small interfering RNA knockdown, where similar MRS results were observed (47). In the breast carcinoma MDA-MB-231 cells, the drop in phosphocholine levels started as early as 4 hours following treatment with MN58b. This was much earlier than the inhibition of cell proliferation and cell cycle arrest, which were only observed following 48 hours of incubation with MN58b. A significant correlation between phosphocholine levels (by MRS) and choline kinase activities

Table 3. *In vitro* magnetic resonance spectroscopy of MDA-MB-231 and HT29 tumor extracts following vehicle control (i.e., saline) and MN58b treatment

Metabolites (μmol/g w wt)	Vehicle	MN58b	*P**
A. ^{31}P-MRS			
MDA-MB-231			
	n = 6	n = 7	
PE	0.79 ± 0.10	0.72 ± 0.12	0.52
PC	0.92 ± 0.08	0.62 ± 0.10	0.04
GPE	0.19 ± 0.10	0.12 ± 0.05	0.54
GPC	0.20 ± 0.10	0.28 ± 0.09	0.60
HT29			
	n = 10	n = 9	
PE	1.40 ± 0.13	1.55 ± 0.11	0.41
PC	2.02 ± 0.24	1.37 ± 0.08	0.03
GPE	0.99 ± 0.06	0.91 ± 0.07	0.36
GPC	1.77 ± 0.17	1.60 ± 0.17	0.45
B. ^{1}H-MRS			
MDA-MB-231			
	n = 5	n = 7	
PC	1.36 ± 0.20	0.83 ± 0.10	0.05
GPC	0.53 ± 0.07	0.47 ± 0.09	0.61
Free choline	0.19 ± 0.08	0.21 ± 0.06	0.92
HT29			
	n = 9	n = 9	
PC	1.70 ± 0.14	1.39 ± 0.07	0.05
GPC	1.62 ± 0.16	1.32 ± 0.16	0.21
Free choline	0.07 ± 0.01	0.11 ± 0.03	0.36

NOTE: Data are expressed as the mean ± SE.
Abbreviations: PE, phosphoethanolamine; PC, phosphocholine; GPE, glycerophosphoethanolamine; GPC, glycerophosphocholine.
*Two-tailed unpaired t-test was used to compare changes between the vehicle- and MN58b-treated groups.

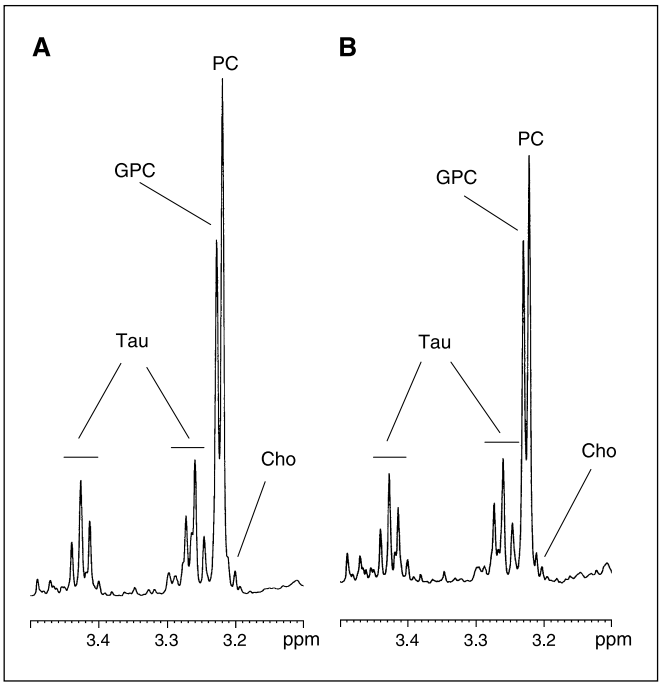

Figure 3. Phosphocholine levels was found to be decreased significantly in the MN58b-treated HT29 tumor extracts when compared with vehicle-treated tumor extracts. Expanded *in vitro* proton (^{1}H)-MRS (3.1-3.5 ppm) of HT29 tumor extracts following treatment with vehicle control (saline; *A*) and MN58b (*B*). Peak assignments were as follows: free choline (*Cho*), phosphocholine (*PC*), glycerophosphocholine (*GPC*), and taurine (*Tau*).

(by ^{14}C labeling) following MN58b treatment (r^2 = 0.95, P = 0.0008) was also found. This indicated that the drop in phosphocholine levels could potentially be used as an early marker for response to choline kinase inhibition in treated tumors. On the other hand, no statistically significant change in phosphocholine levels or cell number was observed in both cell lines following treatment with the chemically related but inactive analogue ACG20b. Overall, our data suggest that the MRS detected drop in phosphocholine is indeed due to the inhibitory effect of MN58b on choline kinase.

Time-response experiments using MDA-MB-231 cells showed an association between the decrease in phosphocholine levels and the length of exposure to MN58b. At 4 hours, phosphocholine levels dropped by 19%, then an average 50% inhibition was detected from 13 to 48 hours of treatment with MN58b. A similar percentage drop in choline kinase activity (54%) was also observed. ^{13}C-MRS comparison of long-term and short-term labeling with [1,2-^{13}C]choline suggested that breakdown of membrane phosphatidylcholine contributed substantially to the phosphocholine levels in MDA-MB-231 breast cancer cells compared with normal human mammary epithelial cells (HMEC; ref. 48). In HMECs, phosphocholine was primarily generated from the action of choline kinase in the biosynthetic pathway. This could result in a slower response to choline kinase inhibition in MDA-MB-231 cells compared with normal HMECs.

Membrane phospholipid metabolism is a cell cycle–regulated event. Phospholipid turnover is high during the G_1 phase, and the accumulation of phospholipid in the S phase correlates with the abrupt cessation of phospholipid turnover at the G_1-S boundary (49). Hence, the effect of MN58b treatment on cell cycle distribution and its relation to the phosphocholine depletion observed was investigated. In attached MDA-MB-231 cells, no statistically significant effect on the cell cycle distribution was detected following treatment with MN58b for up to 30 hours. However, at 48 hours, an accumulation of cells in the G_1 phase is detected with a drop in the cell population in both the S and G_2 phases. The same effect was also observed in HT29 cells following 48 hours of incubation with MN58b. As previously shown (19), MN58b treatment causes inhibition of the *de novo* synthesis of phosphocholine via choline kinase, resulting in a reduction in the total intracellular pool of phosphocholine, which in turn results in a G_1 arrest. Another study has shown that choline deficiency and hence phosphocholine depletion results in the accumulation of fibroblasts in G_1 (50).

There are two phosphatidylcholine biosynthesis pathways in higher eukaryotes, the cytidylyl diphosphate-choline pathway and the methylation pathway. The cytidylyl diphosphate/choline pathway in which choline kinase catalyzes the first phosphorylation reaction, yielding phosphocholine from choline, is the primary route for phosphatidylcholine synthesis in mammals (4). Hence, the effect of phosphocholine depletion following MN58b treatment on phosphatidylcholine biosynthesis was investigated using ^{1}H-MRS of the lipid fractions of control and MN58b-treated MDA-MB-231 and HT29 cells. In keeping with previous metabolic analysis in NIH3T3 cells (18) and human primary lymphocytes (19), no statistically significant changes in phosphatidylcholine levels were detected in attached cell population following treatment of either cell line with MN58b. This could be due to the absolute amount of phosphocholine depletion that we are achieving being low relative to the total pool of phosphatidylcholine, which is the major membrane phospholipid. Furthermore, it is possible that an activation of phosphatidylcholine synthesis via the methylation pathway might have occurred to overcome the drop in phosphatidylcholine synthesis via the cytidylyl diphosphate-choline pathway. Although the methylase is usually not expressed in colon and breast cells, tumor cells could express this enzyme (51). However, our previous results, using either glycerol, choline, or serine labeling as probes, suggest that the methylation pathway is not relevant in this process (19). Quantitative ^{13}C labeling MRS experiments using ^{13}C-labeled choline or ethanolamine would further clarify these observations.

In conclusion, our study showed that MRS can be used to detect a decrease in phosphocholine that is associated with the inhibition of choline kinase by MN58b in human colon and breast carcinoma cell lines. The effects were shown in both cultured cells and in human tumor xenografts. Monitoring the pharmacodynamic effects by MRS (using either ^{31}P or ^{1}H) may provide a noninvasive pharmacodynamic marker for choline kinase inhibition and potentially of tumor response in solid tumors in clinical trials with choline kinase inhibitors.

Acknowledgments

Received 4/17/2005; revised 7/21/2005; accepted 9/16/2005.

Grant support: Cancer Research UK [CUK] grants C1060/A808 (M.O. Leach and L.E. Jackson), C12/A1212/A1209 (Y-L. Chung, J.R. Griffiths, B. Madhu, and H. Troy), and C309/A2187 (P. Workman); Association for International Cancer Research grant 03-304 (N.M.S. Al-Saffar); Spanish Ministerio de Educación y Cultura grant SAF2001-2042 (J.C. Lacal and A. Ramírez de Molina); and Spanish Ministerio de Sanidad y Consumo grants FIS C03-08 and C03-10 (J.C. Lacal and A. Ramírez de Molina).

The costs of publication of this article were defrayed in part by the payment of page charges. This article must therefore be hereby marked *advertisement* in accordance with 18 U.S.C. Section 1734 solely to indicate this fact.

We thank J. Titley for help with flow cytometry analyses.

References

1. Aoyama C, Liao HN, Ishidate K. Structure and function of choline kinase isoforms in mammalian cells. Prog Lipid Res 2004;43:266–81.
2. Exton JH. Signalling through phosphatidylcholine breakdown. J Biol Chem 1990;265:1–4.
3. Kent C. Regulatory and catalytic mechanisms of CTP: phosphocholine cytidylyltransferase. FASEB J 1998;12:58.
4. Kent C. Eukaryotic phospholipid biosynthesis. Annu Rev Biochem 1995;64:315–43.
5. Chung TW, Huang JS, Mukherjee JJ, Crilly KS, Kiss Z. Expression of human choline kinase in NIH 3T3 fibroblasts increases the mitogenic potential of insulin and insulin-like growth factor I. Cell Signal 2000;12: 279–88.
6. Cuadrado A, Carnero A, Dolfi F, Jimenez B, Lacal JC. Phosphorylcholine: a novel second messenger essential for mitogenic activity of growth factors. Oncogene 1993; 8:2959–68.
7. Kiss Z, Tomono M. Wortmannin inhibits carcinogen stimulated phosphorylation of ethanolamine and choline. FEBS Lett 1995;358:243–6.
8. Paulson BK, Porter TJ, Kent C. The effect of polycyclic aromatic hydrocarbons on choline kinase activity in mouse hepatoma cells. Biochim Biophys Acta 1989;1004: 274–7.
9. Ramírez de Molina A, Rodriguez-Gonzalez A, Penalva V, Lucas L, Lacal JC. Inhibition of ChoK is an efficient antitumor strategy for Harvey-, Kirsten-, and N-ras-transformed cells. Biochem Biophys Res Commun 2001;285:873–9.
10. Ratnam S, Kent C. Early increase in choline kinase activity upon induction of the H-ras oncogene in mouse fibroblast cell lines. Arch Biochem Biophys 1995;323: 313–22.
11. Ramírez de Molina A, Gutiérrez R, Ramos MA, et al. Increased choline kinase activity in human breast carcinomas: clinical evidence for a potential novel antitumor strategy. Oncogene 2002;21:4317–22.
12. Ramírez de Molina A, Rodríguez-González A, Gutiérrez R, et al. Overexpression of choline kinase is a frequent feature in human tumor-derived cell lines and in lung, prostate, and colorectal human cancers. Biochem Biophys Res Commun 2002;296:580–3.
13. Hernández-Alcoceba R, Saniger L, Campos J, et al. Choline kinase inhibitors as a novel approach for antiproliferative drug design. Oncogene 1997;15:2289–301.
14. Lacal JC. Choline kinase: a novel target for antitumor drugs. IDrugs 2001;4:419–26.
15. Ramírez de Molina A, Rodríguez-González A, Lacal JC. From Ras signalling to ChoK inhibitors: a further advance in anticancer drug design. Cancer Lett 2004; 206:137–48.
16. Hernández-Alcoceba R, Fernández F, Lacal JC. *In vivo* antitumor activity of choline kinase inhibitors: a novel target for anticancer drug discovery. Cancer Res 1999;59: 3112–8.
17. Ramírez de Molina A, bañez-Coronel M, Gutiérrez R, et al. Choline kinase activation is a critical requirement for the proliferation of primary human epithelial cells and breast tumor progression. Cancer Res 2004;64: 6732–9.
18. Rodríguez-González A, Ramírez de Molina A, Fernández F, et al. Inhibition of choline kinase as specific cytotoxic strategy in oncogene-transformed cells. Oncogene 2003;22:8803–12.
19. Rodríguez-González A, Ramírez de Molina A, Fernández F, Lacal JC. Choline kinase inhibition induces the increase in ceramides resulting in a highly specific and selective cytotoxic antitumoral strategy as a potential mechanism of action. Oncogene 2004;23:8247–59.
20. Gelmon KA, Eisenhauer EA, Harris AL, Ratain MJ, Workman P. Anticancer agents targeting signaling molecules and cancer cell environment: challenges for drug development? J Natl Cancer Inst 1999;91:1281–7.
21. Workman P. Challenges of PK/PD measurements in modern drug development. Eur J Cancer 2002;38: 2189–93.
22. Workman P. How much gets there and what does it do?: the need for better pharmacokinetic and pharmacodynamic endpoints in contemporary drug discovery and development. Curr Pharm Des 2003;9:891–902.
23. Parulekar WR, Eisenhauer EA. Phase I trial design for solid tumor studies of targeted, non- cytotoxic agents: theory and practice. J Natl Cancer Inst 2004;96:990–7.
24. Negendank W. Studies of human tumours by MRS: a review. NMR Biomed 1992;5:303–24.
25. Ronen SM, Leach MO. Imaging biochemistry: applications to breast cancer. Breast Cancer Res 2001; 3:36–40.
26. Leach MO, Verrill M, Glaholm J, et al. Measurements of human breast cancer using magnetic resonance spectroscopy: a review of clinical measurements and a report of localized P-31 measurements of response to treatment. NMR Biomed 1998;11:314–40.
27. Tarnawski R, Sokol M, Pieniazek P, et al. H-1-MRS *in vivo* predicts the early treatment outcome of postoperative radiotherapy for malignant gliomas. Int J Radiat Oncol Biol Phys 2002;52:1271–6.
28. McSheehy PMJ. On the role of MRS in drug development. NMR Biomed 1999;12:402–3.
29. Al-Saffar NMS, Titley JC, Robertson D, et al. Apoptosis is associated with triacylglycerol accumulation in Jurkat T-cells. Br J Cancer 2002;86:963–70.
30. Ronen SM, DiStefano F, McCoy CL, et al. Magnetic resonance detects metabolic changes associated with chemotherapy-induced apoptosis. Br J Cancer 1999;80: 1035–41.
31. Bhakoo KK, Williams SR, Florian CL, Land H, Noble MD. Immortalization and transformation are associated with specific alterations in choline metabolism. Cancer Res 1996;56:4630–5.
32. Smith TAD, Bush C, Jameson C, et al. Phospholipid metabolites, prognosis and proliferation in human breast carcinoma. NMR Biomed 1993;6:318–23.
33. Aboagye EO, Bhujwalla ZM. Malignant transformation alters membrane choline phospholipid metabolism of human mammary epithelial cells. Cancer Res 1999;59:80–4.
34. Ting YLT, Sherr D, Degani H. Variations in energy and phospholipid metabolism in normal and cancer human mammary epithelial cells. Anticancer Res 1996; 16:1381–8.
35. Ronen SM, Jackson LE, Beloueche M, Leach MO. Magnetic resonance detects changes in phosphocholine associated with Ras activation and inhibition in NIH 3T3 cells. Br J Cancer 2002;84:691–6.
36. Sharp SY, Kelland LR, Valenti MR, et al. Establishment of an isogenic human colon tumor model for NQO1 gene expression: application to investigate the role of DT-diaphorase in bioreductive drug activation *in vitro* and *in vivo*. Mol Pharmacol 2000;58:1146–55.
37. Chung YL, Troy H, Banerji U, et al. Magnetic resonance spectroscopic pharmacodynamic markers of the heat shock protein 90 inhibitor 17-allylamino,17-demethoxygeldanamycin (17AAG) in human colon cancer models. J Natl Cancer Inst 2003;95:1624–33.
38. Hotz MA, Gong J, Traganos F, Darzynkiewicz Z. Flow cytometric detection of apoptosis: comparison of the assays of *in situ* DNA degradation and chromatin changes. Cytometry 1994;15:237–44.
39. Workman P, Twentyman P, Balkwill F, et al. United Kingdom Co-Ordinating Committee on Cancer Research (UKCCCR) Guidelines for the Welfare of Animals in Experimental Neoplasia (Second Edition). Br J Cancer 1998;77:1–10.
40. Tyagi RK, Azrad A, Degani H, Salomon Y. Simultaneous extraction of cellular lipids and water-soluble metabolites: evaluation by NMR spectroscopy. Magn Reson Med 1996;35:194–200.
41. Ordidge RJ, Connelly A, Lohman JAB. Image selected *in vivo* spectroscopy (ISIS). A new technique for spatially selective NMR spectroscopy. J Magn Reson 1986;66:283–94.
42. Van der Veen JWC, De Beer R, Luyten PR, Van Ormondt D. Accurate quantification of *in vivo* ^{31}P NMR signals using the variable projection method and prior knowledge. Magn Reson Med 1989;6:92–8.
43. Klose U. *In vivo* proton spectroscopy in presence of eddy currents. Magn Reson Med 1990;14:26–30.
44. Madhu B, Troy H, Robinson SP, Howe FA, Stubbs M, Griffiths JR. Site dependence of choline concentration in HT29 tumours studied by *in vivo* 1H MR spectroscopy [abstract]. Proc Int Soc Magn Reson Med 2003;11:1287.
45. Bergmeyer HU. Methods of enzymatic analysis. Weinheim (Germany): Verlag Chemie; 1974.
46. Workman P, Kaye SB. Translating basic cancer research into new cancer therapeutics. Trends Mol Med 2002;8:S1–9.
47. Glunde K, Raman V, Mori N, Mironchik Y, Bhujwalla ZM. Choline kinase knock-down in breast cancer cells using RNA interference is associated with an increase in intracellular lipid droplets and triacylglycerides [abstract]. Proc Int Soc Magn Reson Med 2004;12:2029.
48. Glunde K, Jie C, Bhujwalla ZM. Molecular causes of the aberrant choline phospholipid metabolism in breast cancer. Cancer Res 2004;64:4270–6.
49. Jackowski S. Coordination of membrane phospholipid synthesis with the cell cycle. J Biol Chem 1994;269: 3858–67.
50. Tercé F, Brun H, Vance DE. Requirement of phosphatidylcholine for normal progression through the cell cycle in C3H/10T1/2 fibroblasts. J Lipid Res 1994;35:2130–42.
51. Walkey CJ, Yu L, Agellon LB, Vance DE. Biochemical and evolutionary significance of phospholipid methylation. J Biol Chem 1998;273:27043–6.